Available online at www.sciencedirect.com
SCIENCE DIRECT
Catalysis Today 104 (2005) 288–295
CATALYSIS TODAY
www.elsevier.com/locate/cattod

Preparation of zeolite-coated pervaporation membranes for the integration of reaction and separation

T.A. Peters [a], J. van der Tuin [a], C. Houssin [a], M.A.G. Vorstman [a], N.E. Benes [a,*], Z.A.E.P. Vroon [b], A. Holmen [c], J.T.F. Keurentjes [a]

[a] *Department of Chemical Engineering and Chemistry, Process Development Group, Eindhoven University of Technology, P.O. Box 513, 5600 MB Eindhoven, The Netherlands*
[b] *Department of Models and Processing, Innovative Materials Group, TNO TPD, P.O. Box 595, 5600 AN, Eindhoven, The Netherlands*
[c] *Department of Chemical Engineering, The Norwegian University of Science and Technology (NTNU), 7491 Trondheim, Norway*

Available online 3 May 2005

Abstract

Pervaporation is a promising option to enhance conversion of reversible condensation reactions, generating water as a by-product. In this work, composite catalytic membranes for pervaporation-assisted esterification processes are prepared. Catalytic zeolite H-USY layers have been deposited on silica membranes by dip-coating using TEOS and Ludox AS-40 as binder material. Membrane pre-treatment and the addition of binder to the dip-coat suspension appear to be crucial in the process. Tuning of catalytic layer thickness is possible by varying the number of dip-coat steps. This procedure avoids failure of the coating due to the high stresses, which can occur in thicker coatings during firing. In the pervaporation-assisted esterification reaction the H-USY coated catalytic pervaporation membrane was able to couple catalytic activity and water removal. The catalytic activity is comparable to the activity of the bulk zeolite catalyst. The collected permeate consists mainly of water and the loss of acid, alcohol and ester through the membrane is negligible. The performance of the membrane reactor is mainly limited by reaction kinetics and can be improved by using a more active catalyst.

Keywords: Esterification; Pervaporation; Catalytic membrane; Zeolite coating; Structured catalyst

1. Introduction

Pervaporation is a promising option to enhance conversion of reversible condensation reactions, generating water as a by-product. Pervaporation is attractive because the energy consumption is low, the reaction can be carried out at the optimal temperature, and the separation efficiency in pervaporation is not determined by the relative volatility as in reactive distillation [1]. In most pervaporation-coupled esterification studies presented so far, the membranes used are catalytically inactive [1–6]. Several authors [7–10], however, used membranes with catalytic activity to carry out esterifications of different alcohols. They showed that equilibrium displacement could be enhanced if the membrane selective layer itself provides the catalytic function. In these studies, however, the membranes were neither very catalytically active nor highly selective to water because one single layer provided both the selective and the catalytic function. Therefore, it has been suggested to use a composite catalytic membrane to be able to optimise both layers independently [10,11]. The principle of an esterification reaction in a composite catalytic membrane reactor is schematically shown in Fig. 1.

The acid and the alcohol molecules diffuse into the catalytic layer where they are converted to an ester and water. The formed ester molecule diffuses back towards the bulk liquid whereas water is removed in situ through the membrane due to the close integration of reaction and separation. Consequently, hydrolysis of the formed ester is reduced and the attained conversion will be increased compared to the inert membrane reactor [7–9]. Additionally, heterogeneous catalysts might be used more efficiently due to the thinness of the catalytic layer present on the membrane support [12]. Other advantages are that no catalyst neutralization or recovery is needed.

* Corresponding author. Tel.: +31 40 2475445; fax: +31 40 2446104.
E-mail address: n.e.benes@tue.nl (N.E. Benes).

0920-5861/$ – see front matter © 2005 Elsevier B.V. All rights reserved.
doi:10.1016/j.cattod.2005.03.065

Nomenclature

k_{obs}	observed reaction rate constant ($m^3\ mol^{-1}\ s^{-1}$)
k_r	reaction rate constant normalized for catalyst amount ($m^3\ mol^{-1}\ g_{cat}{}^{-1}\ s^{-1}$)
t	time (h)
T	temperature (°C)
X	conversion
Subscripts	
c	calcination

The present study focuses on the preparation of composite catalytic pervaporation membranes. The esterification reaction between acetic acid and butanol was taken as a model reaction. First, the activity of various catalysts with respect to the esterification reaction was measured. Subsequently, composite catalytic membranes were prepared by applying a zeolite coating on top of ceramic silica membranes. The goal is to attain a strong and tuneable attachment of zeolite crystals on top of the selective microporous silica layer. Finally, the performance of the composite catalytic membrane as a combined reactor and separator in the esterification reaction was examined.

Zeolite coatings have been used as catalyst in various reactions like condensation, acylation and dehydrogenation reactions [12–17]. Zeolite coating is usually done through a crystallization step where the membrane is soaked in a zeolite crystallization mixture [13]. This method gives a strong attachment and possibly an oriented zeolite layer. However, zeolite crystallization takes place in highly alkaline aluminosilicate solutions. In the present case, direct zeolite crystallization was not possible because the microporous silica layer is not stable under these conditions. As a consequence, a dip-coat method was used. The membrane is immersed at a certain speed in a suspension of zeolite crystals that contains binder material followed by evaporation of the solvent by drying and calcination. Without this binder the deposited crystals will only bind to the surface by "Van der Waals" forces. In the dip-coat technique the resulting catalyst loading is satisfactory and easy controllable. This is important because in the preparation of composite catalytic membranes an optimum in catalytic layer thickness exists [11]. Furthermore, it is not necessary to develop a special zeolite synthesis formulation for coating applications, so an already optimized and catalytically active zeolite can directly be applied.

2. Experimental

2.1. Activity of catalysts

The activity of various zeolites was measured in the esterification of acetic acid and butanol. The zeolites investigated were H-ZSM5 and H-USY and were obtained from Zeolyst Int. (Valley Forge, USA). The average particle size was 1 μm as measured by scanning electron microscopy (SEM). Zeolite H-ZSM5 and H-USY, denoted as H-USY-*x*, where *x* represents the silica to alumina ratio, were used after calcination in an air stream for 8 h at 500 °C. For comparison with the zeolite catalysts also sulphated zirconium oxide was studied. A commercial sulphated zirconium oxide sample was acquired from Mel Chemicals (Manchester, UK) and was used after calcination in an air stream for 6 h at 550 °C.

The catalyst activity was studied in a batch reflux system. A three-necked flask equipped with a condenser and stirrer was charged with acetic acid (0.66 mol) and pre-activated catalyst. Then, the system was heated up to the reaction temperature after which pre-heated alcohol (0.66 mol) was added. The reaction temperature was maintained by means of a thermostatic water bath in which the reactor was immersed. For kinetic measurements, samples were taken periodically and analysed by a gas chromatograph equipped with a flame ionisation detector and a thermal conductivity detector. All catalysts were employed under similar reaction conditions. The reaction was performed at a temperature of 75 °C. GC analysis confirmed that no by-products were formed. The reaction rate constants were evaluated from the measured time-dependent concentration curves using the differential method. The non-linear least-squares regression technique was used to minimise the sum of the square differences on the reaction rate for acetic acid.

2.2. Coating and testing of the pervaporation membranes

Ceramic pervaporation hollow fibre membranes (TNO-TPD, The Netherlands) were used. The inner and outer diameter of the membranes is 2.0 mm and 3.2 mm, respectively. The length of the membranes is 20 cm. They consist of γ-alumina layers supported on a porous α-alumina tubular membrane. The permselective layer on the outside of the support is a thin (70 nm) layer made of microporous amorphous silica [18]. In the dehydration of *n*-butanol these membranes have proved to combine a high water flux with a good selectivity [18].

2.3. Standard binder solution

A silica binder solution was prepared as follows: TEOS (Merck, >98%) was mixed with ethanol and water. A small amount of nitric acid (65 wt.% in water) as a silicate oligomerisation catalyst was added and the resulting mixture was heated at 60 °C for 3 h under continuous stirring. The reaction mixture had a molar ratio TEOS/ethanol/water/HNO_3 of 1/3.8/6.4/0.085. Commercial colloidal silica (Ludox AS-40, Aldrich) was also used as a binder solution.

2.4. Zeolite dip-coat suspensions

The dip-coat solutions were prepared by mixing H-USY crystals and ethanol. Dealuminated zeolite H-USY with a

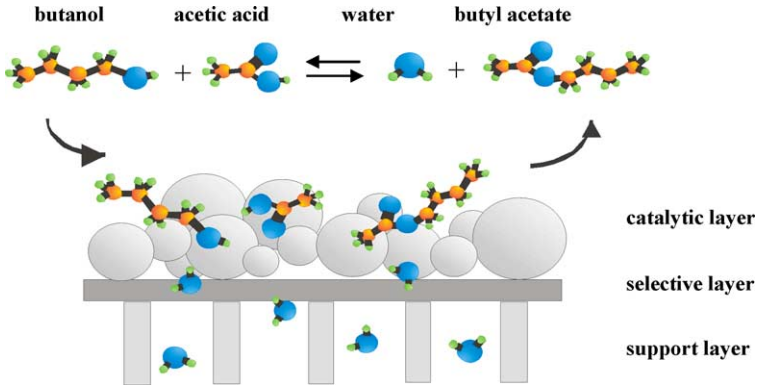

Fig. 1. Schematic representation of the esterification reaction between acetic acid and butanol in a composite catalytic membrane reactor.

Si/Al ratio of 40 was selected for the coating experiments. The Na_2O content was 0.05 wt.% and the surface area 650 $m^2\,g^{-1}$. The amount of zeolite crystals was varied between 5 wt.% and 26 wt.%. The suspensions were sonicated at room temperature for 1 h prior to use. 10 wt.% of standard binder solution was added to the zeolite dip-solution to enhance particle deposition and layer strength.

2.5. Dip-coat process

Membranes were first immersed (16 mm s^{-1}) in the binder solution for 2 min and removed from the binder solution at the same speed. Next, membranes were dipped into a zeolite suspension for 2 min (longer times did not significantly change the final loading) at a speed of 16 mm s^{-1}. Typically, the zeolite dip-coat procedure started 1 min after the pre-treatment. Subsequently, the membranes were dried in air at 60 °C for 2 h and calcined for 16 h in air at 500 °C with a heating rate of 100 °C h^{-1}.

2.6. Characterization

The loading of zeolite crystals on the membrane surface was determined by the weight increase during the dip-coating process. The adhesion of zeolite crystals was tested by an ultrasonic bath treatment for 1 h followed by scanning electron microscopy to evaluate the amount of crystals remaining at the surface. SEM pictures were taken using a JEOL JSM-5600 with an acceleration voltage of 15 kV. Dry coated membrane samples were gold-coated prior to scanning.

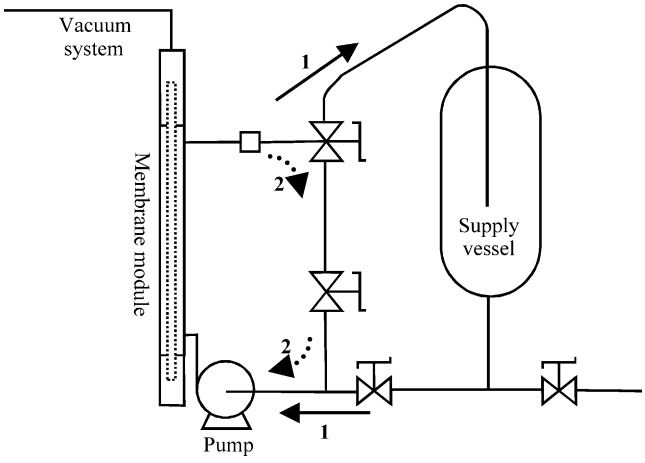

Fig. 2. Set-up used in the catalytic tests and the pervaporation–esterification coupling.

2.7. Catalytic test

The activity of the zeolite-coated pervaporation membrane was measured in the esterification reaction between acetic acid and butanol under the same reaction conditions as mentioned above in the catalyst screening experiments. The membrane was placed in a stainless steel module using Kalrez® O-rings. Effective membrane area used was 17 cm^2. The set-up used is depicted in Fig. 2.

The supply vessel was charged with a certain amount of acetic acid. Then, the system was heated up to the reaction temperature ($T = 75$ °C) after which the pre-heated equimolar amount of alcohol was added. The reaction temperature was maintained by means of a thermostatic water bath in which the system was immersed. The liquid reaction mixture was recirculated through the membrane module by means of the pump (valves are in position 1) at a liquid flow rate of 40 l h^{-1}, which corresponds to a liquid superficial velocity exceeding 2 m s^{-1} in order to eliminate polarization effects. On the permeate side a vacuum was maintained (10 mbar) by a cascade of a liquid nitrogen cold trap and a vacuum pump. After recirculation through the membrane module, the flow towards the supply vessel was stopped, decreasing the reactor volume to 30 ml, and the liquid was only flowing through the membrane module containing the catalytic membrane (valves are in position 2).

3. Results

3.1. Activity of heterogeneous catalysts

All experiments showed first-order behaviour in acetic acid and butanol concentration. The activity of the catalysts

Table 1
Activity of the different catalysts in the esterification reaction between acetic acid and butanol, $T = 75\ ^{\circ}C$

Catalyst	Amount (g)	T_c (°C)	k_{obs} ($m^3\ mol^{-1}\ s^{-1}$)	k_r ($m^3\ mol^{-1}\ g_{cat}^{-1}\ s^{-1}$)	X ($t = 2$ h)
No catalyst	–	–	1.3×10^{-9}	–	0.07
H-USY-20	2.88	500	2.8×10^{-9}	9.8×10^{-10}	0.19
H-ZSM5-12.5	2.82	500	1.7×10^{-10}	5.9×10^{-11}	0.08
ZrO_2	5.01	550	4.4×10^{-8}	8.8×10^{-9}	0.56

is expressed in terms of the second-order reaction rate constant normalised for the catalyst weight. As the reaction also proceeds without adding a catalyst, the first-order reaction rate constant of this reaction is also given. The results are shown in Table 1.

Large-pore zeolites, like X and Y-type zeolites have proven to be efficient catalysts for esterification reactions [19,20]. Zeolite catalytic properties like pore size, acid strength distribution and hydrophobicity can be designed by preparing zeolites with different crystalline structure, acid exchange level and framework Si/Al ratio. For example, with increasing Si/Al ratios, the zeolite surface becomes more hydrophobic and, therefore, has more affinity for the reactants, whereas the number of acid sites decreases. Hence, an optimum Si/Al ratio may exist. Fig. 3 shows the influence of the zeolite Si/Al ratio for H-USY on the zeolite activity in the esterification reaction between acetic acid and butanol.

The highest activity for the H-USY zeolite activity was found at a Si/Al ratio of around 20. This agrees with the value obtained by Corma et al. [20] for the esterification of carboxylic acids in the presence of HY zeolites. H-ZSM5 had the lowest activity of the catalysts tested suggesting that the esterification is internally diffusion-limited due to the medium sized H-ZSM5 zeolite pores [19]. Thus, most of the conversion occurs on the external surface of the crystallites.

The activity and stability of sulphated zirconia towards the esterification reaction highly depends on the catalyst pre-treatment. At increasing calcination temperature, the crystallinity of the sulphated zirconia increases, whereas the surface area and the amount of surface sulphur species

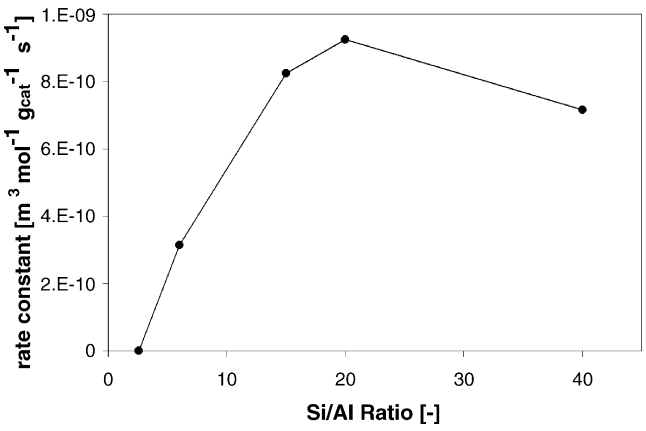

Fig. 3. Effect of the H-USY Si/Al ratio on the activity in the esterification reaction between acetic acid and butanol, $T = 75\ ^{\circ}C$.

decreases [21]. Hence, an optimum in reactivity as a function of calcination temperature may exist. This optimum was found at a calcination temperature of 550 °C. This agrees with the optimum calcination temperature obtained by Hino and Arata [22] for the esterification reaction of acetic acid and ethanol in the presence of sulphated zirconia. From Table 1 it can be seen that the weight based activity of sulphated zirconia exceeded the activity of the two zeolites tested. However, due to water adsorption on the active sites or loss of surface sulphur sites, the activity of sulphated zirconia gradually decreased. Additionally, for the regeneration of this type of catalysts multiple steps are needed whereas for regeneration of zeolites only calcination in air has to be performed [22]. Therefore, H-USY zeolite is considered to be the most suitable catalyst to be applied as the catalytic layer in a catalytic membrane reactor.

3.2. Coating of the ceramic pervaporation membranes

3.2.1. Ludox As-40 as binder

Commercial reactive colloidal silica nanoparticles such as Ludox AS-40 (40 wt.% suspension of colloidal silica in water) are commonly used as binder to enhance zeolite crystal attachment on aluminosilicate substrates [13–16]. From Fig. 4 it can be seen that after pre-treatment of the membrane surface in a Ludox AS-40 solution, zeolite attachment was increased dramatically.

Discontinuous zeolite coverage is clearly observed. However, the most interesting feature is that a Ludox layer is required to enable zeolite crystals to be attached to the surface. Fig. 4b shows a Ludox layer of approximately 0.5 μm between the zeolite crystals and the selective silica layer of the membrane. Where there are no AS-40 particles (or very few) virtually no attachment is observed. This signifies how important pre-treatment of the membrane surface is for zeolite adhesion. The difficult attachment could be ascribed to the fact that the original membrane surface probably does not contain enough reactive sites to induce chemical attachment or does not exhibit enough surface roughness to induce physical attachment. Unfortunately, a full coverage could not be achieved and the zeolite layer was unstable under ultrasonic treatment. Therefore, oligomeric silica particles were considered as binder to enhance zeolite attachment and zeolite layer strength. Such a binder should not form a thick layer unlike the above-mentioned results, which could be detrimental to permeation. Additionally, a better membrane coverage is expected as the reactivity of TEOS is higher compared to Ludox AS-40.

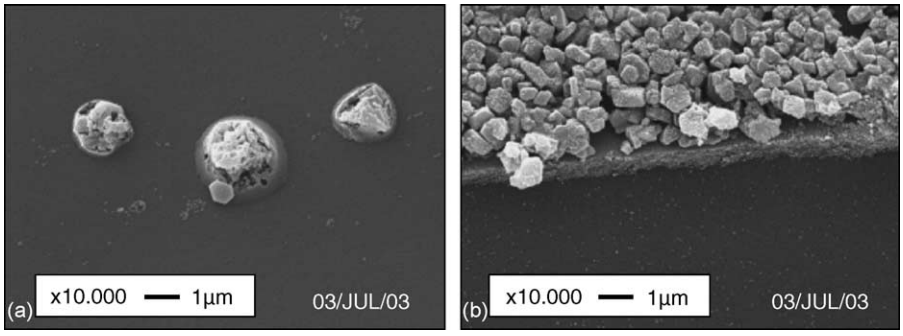

Fig. 4. SEM pictures of a H-USY zeolite-coated membrane (top view), prepared with a 20 wt.% H-USY mixture in ethanol: (a) without pre-treatment; (b) with pre-treatment in a Ludox AS-40 binder solution.

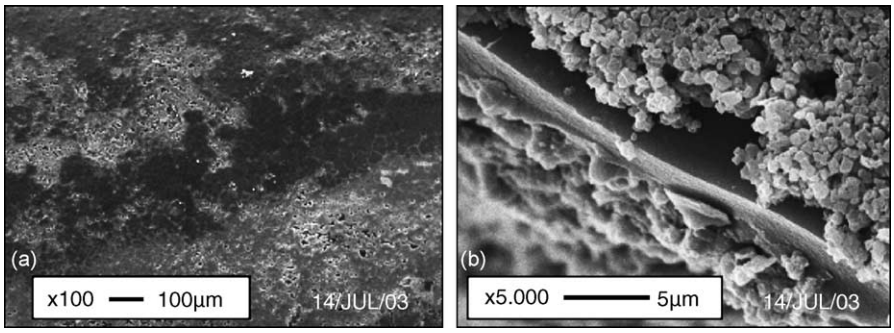

Fig. 5. SEM pictures of a H-USY zeolite-coated membrane, prepared with a 20 wt.% H-USY mixture in ethanol pre-treated in a TEOS solution: (a) top view; (b) side view.

3.2.2. *Oligomeric silica as binder*

Fig. 5 shows a zeolite-coated membrane obtained from a 20 wt.% zeolite dip-coat solution after pre-treatment in a 10 wt.% TEOS binder solution. It can be seen that a crack-free zeolite layer was obtained. The coverage is improved as compared to the membrane pre-treated in a Ludox AS-40 binder solution.

Coating a membrane once in a coating mixture of 20 wt.% H-USY resulted in a zeolite layer thickness of around 2 μm after calcination as seen by SEM, later confirmed using a profilometer. The amount of zeolite deposited on the membrane can be predicted from the solution film thickness that should remain on the surface upon withdrawal from the zeolite solution; on the basis of viscosity, surface tension, density, and the speed of withdrawal, the resulting zeolite layer thickness for a single withdrawal should be 3 μm [23]. This prediction agrees well with our experimental results. A significant amount of zeolite remains on the surface after 1 h of sonication, which indicates firm attachment of the zeolite layer. In order to increase zeolite layer strength, 10 wt.% of binder was added to the dip-coat solution. The influence of this binder on the zeolite layer is clearly visible from Fig. 6. Due to the presence of binder in the dip-coat solution, separate zeolite particles in the zeolite layer are intergrown and the resulting zeolite layer is strengthened.

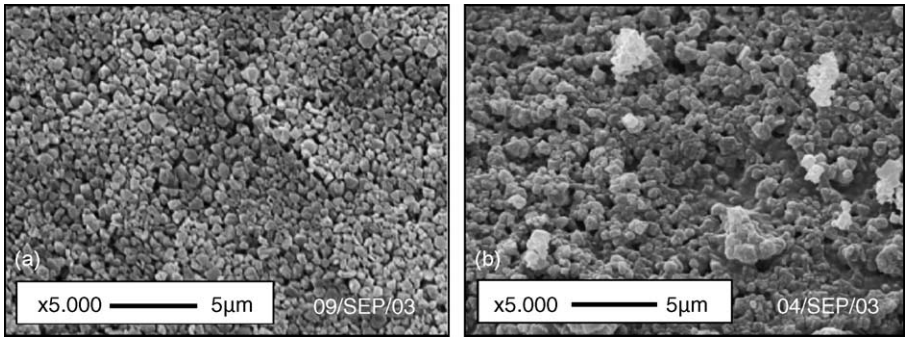

Fig. 6. SEM pictures of a H-USY zeolite-coated membrane, prepared with a 20 wt.% H-USY mixture in ethanol pre-treated in a TEOS solution: (a) no binder in dip-coat solution; (b) 10 wt.% binder in dip-coat solution.

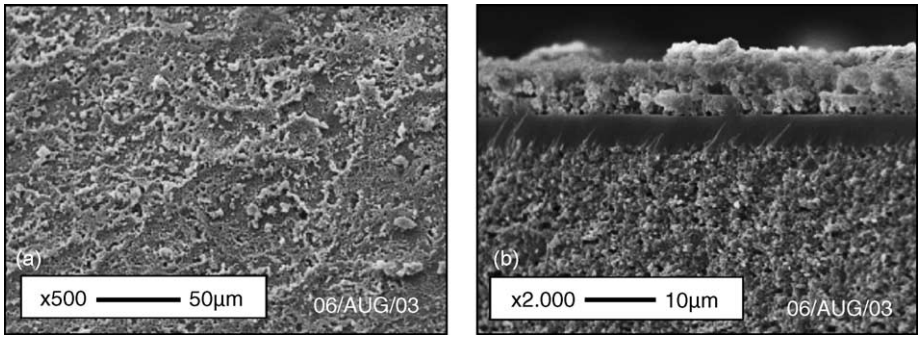

Fig. 7. SEM pictures of a H-USY zeolite-coated membrane, prepared with a 20 wt.% H-USY mixture in ethanol pre-treated in a TEOS solution, procedure repeated four times: (a) top view; (b) side view.

Varying the zeolite concentration in the coating mixture between 3 wt.% and 20 wt.% did not seem to affect the final layer thickness substantially. In more concentrated mixtures the zeolite layer thickness increased dramatically. In these thick layers, however, cracks appeared during drying and the layer was easily removed during the ultrasonic treatment. Therefore, in order to increase the layer thickness, the dipping procedure was repeated four times. This deposition method avoids failure of the coating due to the high stresses, which can form in thicker coatings during drying or firing. A calcination step has been applied after every dip-coat experiment. The results are presented in Fig. 7.

From Fig. 7b it can be observed that the zeolite layer thickness is approximately 10 μm (5 × 2 μm). The coverage is uniform as shown in Fig. 7a. Hence, tuning of the zeolite coating thickness is possible by varying the number of dip-coat steps.

3.3. Activity of the zeolite-coated ceramic pervaporation membranes

The catalytic function of the H-USY coated pervaporation membrane combined with its selective features was tested in the esterification reaction between acetic acid and butanol. For this, a membrane is selected which is dip-coated ten times resulting in a layer thickness of around 40 μm. Zeolite coverages up to 10 g m^{-2} of membrane area, which translates to reactor loadings of zeolite up to 80 kg m^{-3} of reactor volume were obtained. The activity of the coated membrane was compared to the activity obtained for the bulk zeolite catalyst. In both reactions the (initial) observed rate constants and intrinsic rate constants per gram of zeolite are in the same order of magnitude. The coated membrane exhibits an activity of 9.2×10^{-10} m^3 mol^{-1} s^{-1} $g_{cat}{}^{-1}$, which is only 7% lower than the value given in Table 1. Most likely, inhibition of external acid sites by the TEOS binder is the explanation for the somewhat lower activity [24]. However, due to the relatively low amount of catalyst compared to the area-to-volume ratio of the experimental set-up (<100 m^2 m^{-3}, instead of 1000 m^2 m^{-3} in a practical membrane module), a substantial conversion could not be reached within a reasonable time scale (typical 80 mg of catalyst coated on a membrane with a length of 20 cm and a reactor volume of 30 ml). Therefore, it was chosen to use a feed at equilibrium conversion. This feed simulates the outlet stream from a conventional reactor, with an equimolar feed mixture at equilibrium conversion. The results are shown in Figs. 8–10.

From Fig. 8 it can be seen that initial water removal from the reactor is high, which shows the selective function of the membrane. After 3 h the excess of water in the reactor is removed suggesting that the performance of the membrane

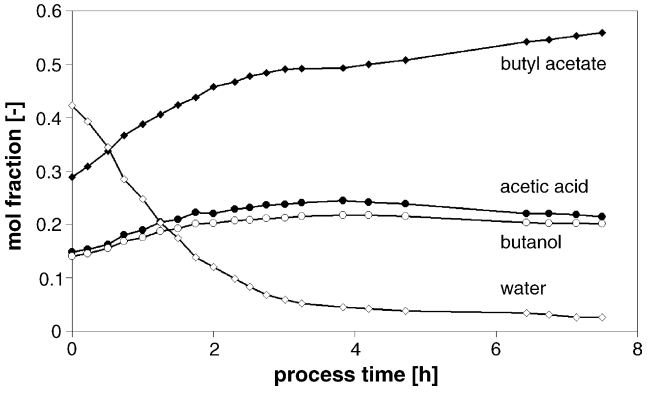

Fig. 8. Mole fractions in the composite catalytic membrane assisted esterification of acetic acid and butanol as a function of time, $T = 75$ °C.

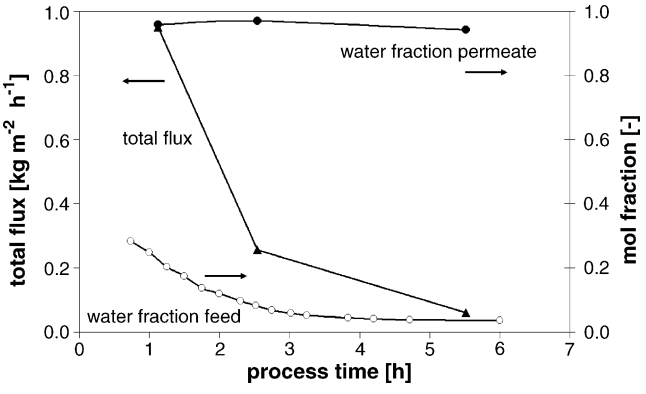

Fig. 9. Total flux through the composite catalytic membrane and water fraction in the feed and permeate, respectively, $T = 75$ °C.

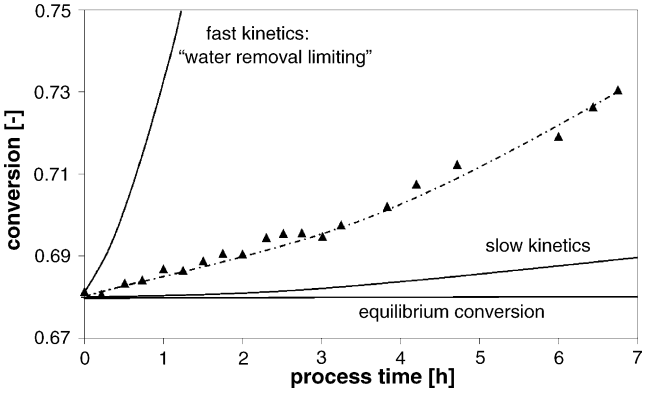

Fig. 10. Conversion of acetic acid in the composite catalytic membrane assisted esterification of acetic acid and butanol (▲), $T = 75$ °C. Dashed line is a guide to the eye.

reactor is mainly limited by the reaction kinetics. From this stage, the water production due to reaction equals the water removal from reaction and thus, the water fraction is constant. In contrast to other studies [7,9], the collected permeate consists mainly of water indicating the beneficial effect of the dual-layer structure. Thus, reactant and product loss through the membrane are negligible as can be seen from Fig. 9. The total flux through the membrane decreases in time mainly due to the decreasing water fraction in the reactor as can be seen from Fig. 9. Fig. 10 shows the conversion plotted against time for a catalytic membrane reactor. The simulated curves present two extreme cases: the system is limited by either reaction kinetics or by water removal. For the simulations regarding the water removal limited case, the reaction rate constant is chosen such that further increase did not alter the conversion behaviour. For the case that the reaction kinetics are limiting, the curve is obtained using the reaction rate constant for the uncatalysed reaction given in Table 1 assuming first-order reaction kinetics for both the reactants [11].

Fig. 10 shows that the reached conversion of the catalytic membrane-assisted esterification reaction clearly exceeds thermodynamic equilibrium. It can also be seen that the performance of the catalytic membrane is indeed limited by kinetics and that the reached conversion can be improved substantially by using a more active catalyst. Furthermore, one should realize that applied area-to-volume ratio and catalyst amount are easily controllable by applying multiple membranes in one single module and consequently it is conceivable that an improved performance can easily be realized.

4. Conclusions

Composite catalytically active membranes can be used to enhance conversion of esterification reactions as the reaction and separation function are coupled very efficiently. An additional advantage is that both the selective layer and the catalytic layer can be optimised independently. In this work, composite catalytic membranes are prepared by a dip-coating technique. Catalytic zeolite H-USY layers have been deposited on silica membranes using TEOS as well as Ludox AS-40 as binder. Membrane pre-treatment and the addition of binder to the dip-coat suspension appear to be crucial in the dip-coat process. Varying the zeolite concentration in the coating mixture between 3 wt.% and 20 wt.% did not seem to affect the final layer thickness. Tuning of catalytic layer thickness is possible by varying the number of dip-coat steps. This procedure helps to avoid failure of the coating due to high stresses that can occur in thicker coatings during drying and firing. In the pervaporation-assisted esterification reaction the catalytic membrane was able to couple catalytic activity and water removal. The catalytic activity of the H-USY coated catalytic pervaporation membrane was comparable to the activity of the bulk zeolite catalyst. The collected permeate consists mainly of water and thus, acid, alcohol and ester loss through the membrane are negligible. The performance of the system can be improved by using a more active catalyst.

Acknowledgements

This work was performed in a cooperative project of the Centre for Separation Technology and was financially supported by TNO and NOVEM. We would like to thank Henk Woestenberg for taking the SEM pictures.

References

[1] D.J. Benedict, S.J. Parulekar, S.-P. Tsai, Ind. Eng. Chem. Res. 42 (2003) 2282.
[2] J.T.F. Keurentjes, G.H.R. Janssen, J.J. Gorissen, Chem. Eng. Sci. 49 (1994) 4681.
[3] Y. Zhu, R.G. Minet, T.T. Tsotsis, Chem. Eng. Sci. 51 (1996) 4103.
[4] L. Domingues, F. Recasens, M. Larrayoz, Chem. Eng. Sci. 54 (1999) 1461.
[5] R. Krupiczka, Z. Koszorz, Sep. Purif. Technol. 16 (1999) 55.
[6] Q.L. Liu, Z. Zhang, H.F. Chen, J. Membr. Sci. 182 (2001) 173.
[7] M.O. David, T.Q. Nguyen, J. Neel, J. Membr. Sci. 73 (1992) 129.
[8] L. Bagnell, K. Cavell, A.M. Hodges, A.W. Mau, A.J. Seen, J. Membr. Sci. 85 (1993) 291.
[9] M.P. Bernal, J. Coronas, M. Menéndez, J. Santamaría, Chem. Eng. Sci. 57 (2002) 1557.
[10] Q.T. Nguyen, C.O. M'Bareck, M.O. David, M. Métayer, S. Alexandre, Mater. Res. Innovat. 7 (2003) 212.
[11] T.A. Peters, J. Fontalvo, M.A.G. Vorstman, J.T.F. Keurentjes, Chem. Eng. Res. Des. 82 (2004) 220.
[12] T. Vergunst, F. Kapteijn, J.A. Moulijn, Ind. Eng. Chem. Res. 40 (2001) 2801.
[13] J.C. Jansen, J.H. Koegler, H.P.A. Calis, C.M. van den Bleek, F. Kapteijn, J.A. Moulijn, E.R. Geus, N. van der Puil, Microporous Mesoporous Mater. 21 (1998) 213.
[14] A.E.W. Beers, R.A. Spruijt, T.A. Nijhuis, F. Kapteijn, J.A. Moulijn, Catal. Today 66 (2001) 175.

[15] T.A. Nijhuis, A.E.W. Beers, F. Kapteijn, J.A. Moulijn, Chem. Eng. Sci. 57 (2002) 1627.
[16] A.E.W. Beers, R.A. Spruijt, T.A. Nijhuis, F. Kapteijn, J.A. Moulijn, Microporous Mesoporous Mater. 48 (2001) 279.
[17] S.M. Lai, R. Martin-Aranda, K.L. Yeung, Chem. Commun. 2 (2003) 218.
[18] T.A. Peters, J. Fontalvo, M.A.G. Vorstman, N.E. Benes, R.A. van Dam, Z.A.E.P. Vroon, E.L.J. van Soest-Vercammen, J.T.F. Keurentjes, J. Membr. Sci. 248 (2005) 73.
[19] S. Namba, Y. Wakushima, T. Shimizu, T. Yashima, Stud. Surf. Sci. Catal. 20 (1985) 205.
[20] A. Corma, H. Garcia, S. Iborra, J. Primo, J. Catal. 120 (1989) 78.
[21] J. Hu, C. Wei, F. Qiu, Z. Xu, Q. Chen, J. Nat. Gas Chem. 9 (2000) 212.
[22] M. Hino, K. Arata, Chem. Lett. (1981) 1671.
[23] W.B. Lacy, L.G. Olsen, J.M. Harris, Anal. Chem. 71 (1999) 2564.
[24] P.J. Kunkeler, D. Moeskops, H. van Bekkum, Microporous Mater. 11 (1997) 313.